

University Turbines Systems Research (UTSR)
2012 Gas Turbine Industrial Fellowship Program

**CFD POST PROCESSING OF INDUSTRIAL GAS TURBINE
EXHAUST DIFFUSER
AND
OPTIMIZATION OF A ONE DIMENSIONAL ANALYSIS TOOL**

Prepared For:

SIEMENS

Siemens Energy
Orlando, FL 32826

&

SwRI[®]

Southwest Research Institute
San Antonio, TX 78228

Prepared by:

Leolein P. Moualeu
University of North Dakota
Grand Forks, ND 58203

I. INTRODUCTION

Land-based gas turbines have large amounts of kinetic energy at the last turbine stage. Exhaust diffusers downstream of the last stage convert some of this energy into additional static pressure at the diffuser outlet. Since the diffuser exit pressure is set by the ambient condition (exhaust stack), the static pressure at the diffuser inlet, hence at the turbine exit, is lowered. This low static pressure enhances the power of the turbine and the thermal efficiency whether the gas turbine is used in simple cycle or combined cycle application.

In a quest to address today's increasing demand for higher gas turbine performances, Siemens has conducted extensive researches about the geometrical effects and the impact of inlet conditions on exhaust diffusers. Findings of these researches needed to be summarized in a standard format that would be beneficial for future diffuser improvements. Numerical results of several real exhaust diffusers, for different gas turbine fleet, were post processed and gathered in catalogue format. This report describes similar effort done on CFD model representing the baseline configuration test rig, built at the Institute of Thermal Turbomachinery and Machinery Laboratory of the University of Stuttgart, Germany (ITSM).

CFD simulations are common practice to predict the flow complexity of exhaust diffusers. High-fidelity CFD models can require millions of meshes for which conservation of mass, momentum and energy are calculated in every one of these cells. However, the computational challenge and the mesh load of numerical modeling can be an uneconomical use of resources. Development of a relatively accurate and economic one-dimensional (1D) tool has been started. The 1D tool is designed to give preliminary insight of the diffuser geometry and first assessment of the overall diffuser performance. Designs showing promising results will be validated for further CFD analyses and experimental investigations.

II. EXHAUST DIFFUSER CATALOGUE

The diffuser catalogue, a database of relevant information about the diffuser geometry and performance for pre-determined flow conditions, was partly built from CFD simulations. Post processing of simulation results was conducted using ANSYS CFX-Post. Figure 1 shows the computational domain representing half of the baseline configuration of the ITSM test rig. The diffuser inlet was chosen a few centimeters downstream of the main inlet. The model also displays two and half of the five radial struts with an exhaust stack downstream of the conical segment.

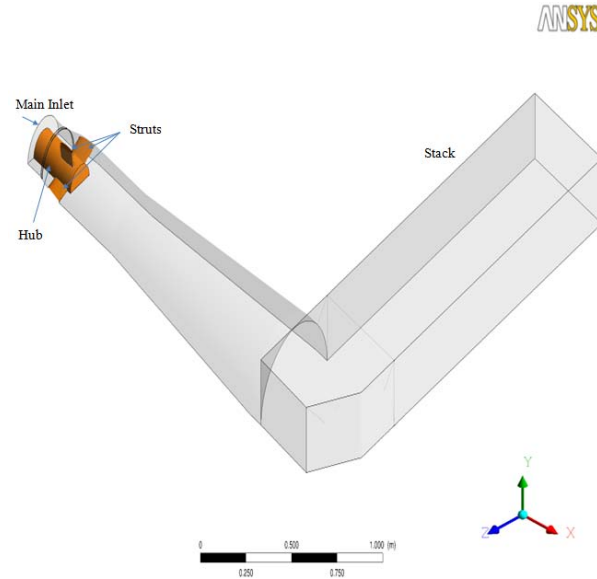


Figure 1. Baseline Configuration of ITSM Test Rig

The catalogue contains three main sections to characterize the diffuser. The first section gathers the geometries of the exhaust diffuser and the last turbine blade. The second section shows the inlet boundary conditions of the diffuser. Some important parameters defined at the diffuser inlet are total pressure and total temperature, the Mach number, the swirl and pitch angles. This section also displays the strut profiles and the calculated pressure coefficients. The third section shows the diffuser performances and losses. The exit conditions are presented in this section by the use of total pressure and total temperature contours, and also velocity contours.

A. Geometry section

Standard views of the diffuser geometry with complete dimensions can be collected from CAD drawings (cold geometry). Typically, CFD models represent the geometry during continuous operation (hot geometry). Having both geometries displayed in this section of the catalogue can help capture the radial growth and the axial displacement of the exhaust components. Figure 2 shows a schematic of the diffuser with the diffuser inlet depicted by a radial plane positioned at the last turbine blade trailing-edge. This definition of the inlet was convenient for proper geometry and flow parameter input in the 1D analysis tool.

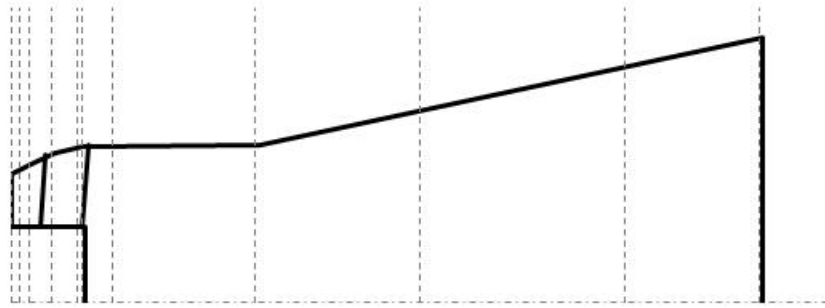
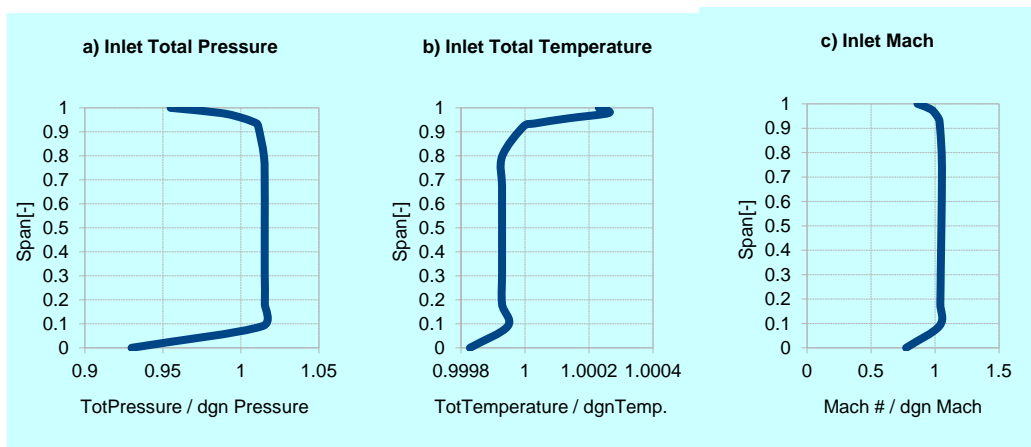


Figure 2. Schematic of ITSM Diffuser for the Baseline Configuration with Radial Plane Locations for Performance Calculations

B. Aerodynamic section

The diffuser inlet profiles were defined with the total pressure and total temperature, the swirl and pitch angles, the axial tangential and radial velocities. These profiles were calculated at thirteen radial locations using circumferential averaging. Mean values of flow properties at the diffuser inlet, summarized in a table, also included some aerodynamic parameters such as the inlet Mach number and the shape factor. These values were mostly mass averaged with the exception of the static pressure and static temperature which were area averaged. Figure 3 shows the diffuser inlet profiles of the baseline configuration. For reasons of confidentiality the inlet profiles and the performance of the diffuser (displayed in Figure 4) are shown relative to respective reference values (or design values). Information regarding the load on the struts was included in this section of the catalogue. The variation of the pressure coefficient along the strut axial chord was calculated at the location near the hub, at the mid span, and close to the casing.



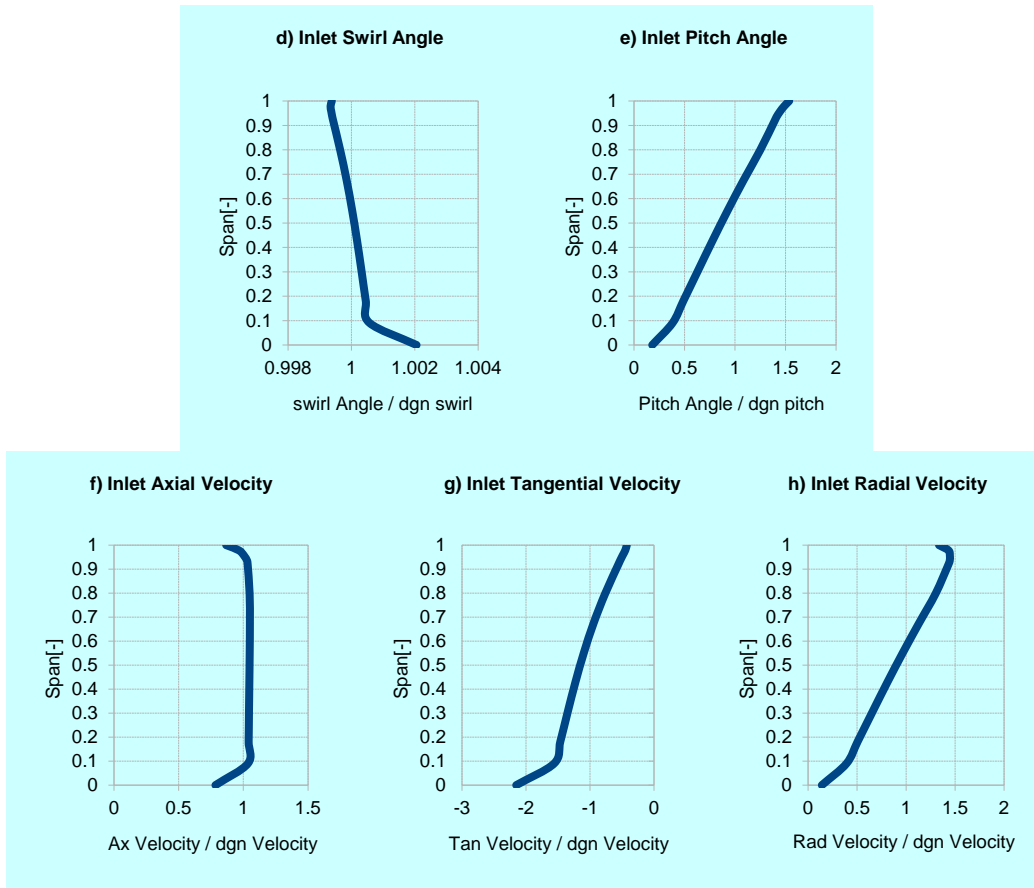


Figure 3. Inlet Profiles of ITSM Diffuser for the Baseline Configuration

C. Performance section

The performance of the exhaust diffuser can be evaluated by calculating the pressure recovery. The pressure recovery and the area ratio calculations were incrementally monitor, along the diffuser, to capture the geometry blockage and the drop of the static pressure at the strut leading edge. The performance section also included calculations of total pressure loss coefficient, kinetic energy coefficient, total pressure drop, and the static pressure of the diffuser. These calculations were done at different plane locations as displayed in Figure 2. Some of the calculated parameters of the baseline diffuser are shown in Figure 4. Boundary conditions at the diffuser exit were also presented in this section of the catalogue with contour plots of total pressure, total temperature and velocity. Different load conditions (part loads) can be applied on a single diffuser geometry for simulation. Variations of the inlet profile at different loads were estimated by plotting the total and static pressure against the swirl angle and the Mach number.

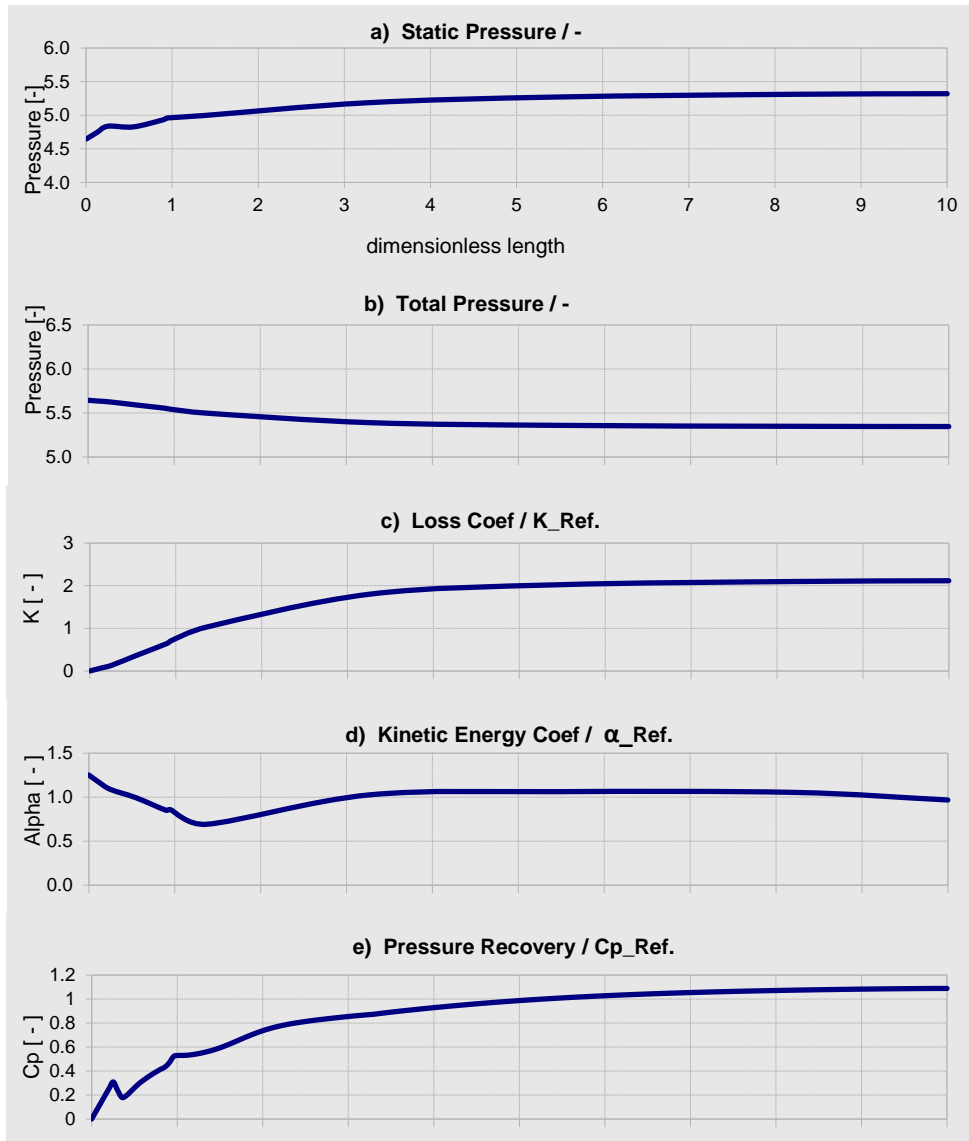


Figure 4. Performances and Losses along ITSM Diffuser for the Baseline Configuration

A reference sheet locating the sources that were used to develop the catalogue was included in the formatting. This sheet will also include the definition or formulation of some of the calculations such as the pressure recovery and the blockage.

III. OPTIMIZATION OF ONE DIMENSIONAL DIFFUSER ANALYSIS TOOL

A. Overview

The Performance of an exhaust diffuser, for stationary gas turbines, is influenced by the inlet profiles and the geometrical shape of the diffuser. The 1D tool was built around

these two factors by requiring input of flow conditions at the trailing edge of the last turbine stage and input of the geometry parameters. This flow calculator was developed in a spreadsheet format to simplify its implementation and development. The first sheet (or tab) gathered the necessary fluid properties at the inlet, along with flow properties such as the mass flow rate, the Reynolds number, and the initial pressure recovery. The second tab of the tool was reserved for the diffuser geometry inputs. These inputs were used to calculate 2D coordinates and generate a schematic of the designed diffuser. Figure 5 shows the ITSM diffuser as modeled in the 1D tool. The number of calculation tabs vary according to the number of divisions applied on the diffuser. In the present case, the ITSM diffuser was segmented in four regions: an annular region, a strut region, a hub-end region, and a conical region. Since the physics applied in these regions might differ, each region calculations were computed separately.

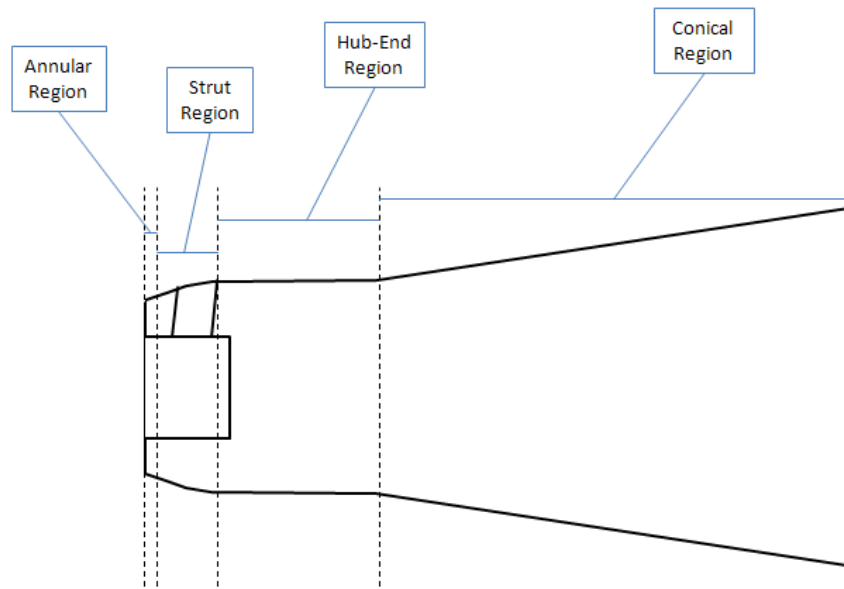


Figure 5. 1D-tool Modeling of ITSM Diffuser for the Baseline Configuration

The annular region represents the zone between the last turbine stage trailing edge to a few centimeters upstream of the strut leading-edge. The required geometry parameters were limited to the inner and outer diameter at the region inlet ($d_{h,1}$ and $d_{ip,1}$), the axial length of the region (L), the diverging angle at the wall, and the diverging angle at the hub (θ_{OD} and θ_{ID}).

The strut region has the most required geometry parameters, due to the strut presence and orientation, and a second diffusing angle at the diffuser wall. In addition to the parameters mentioned for the annular region, inputs such as the number of struts (n_s), the pitch angle (θ_p), the dihedral angle (θ_d) for the strut orientation (radial or tangential), the airfoil maximum thickness (d_s) and length of the strut (L_s), were also required in this region.

Virtually all axial exhaust diffusers have a step at the end of the hub as it can be seen in Figure 5. The hub length (L_h) was an important input parameter in hub-end region to accurately calculated the sudden area expansion.

The conical region required less parameter input due to the absence of a hub. This segment of a diffuser can have more than one diffusing angle depending on the design. A typical conical region with one diffusing angle is display in Figure 5.

B. Diffuser Calculations

1D flow permits simplification of the governing fundamental laws along a straight diffuser. The calculations done in the tool do not account for heat transfer, assuming steady incompressible flow. The momentum equation applied in the four regions illustrated in Figure 5, is computed as follow:

$$p_1 \cdot A_1 - p_2 \cdot A_2 - \sum F_{drag} + F_p = \rho \cdot (-A_1 \cdot c_{x,1}^2 + A_2 \cdot c_{x,2}^2) \quad (\text{Eq. 1})$$

The region outlet velocity $c_{x,2}$ is calculated using the conservation of mass

$$A_1 \cdot c_{x,1} = A_2 \cdot c_{x,2} \quad (\text{Eq. 2})$$

The wall pressure forces combine both the pressure force at the casing and the hub

$$F_p = \left(\frac{p_1 + p_2}{2} \right) \cdot (A_{p,w} \cdot \sin \theta_{OD} - A_{p,h} \cdot \sin \theta_{ID}) \quad (\text{Eq. 3})$$

where $A_{p,w}$ and $A_{p,h}$ are the planform areas at the casing and the hub, respectively.

Drag predictions, implemented in the tool, were dependent on the flow complexity for each region. For the annular and the conical regions, the drag sources were attributed to the skin-friction drags at the casing and the hub. The Prandtl Schlichting correlation (1932) was used to estimate losses due to skin-friction drag

$$\overline{C_f} = \frac{0.455}{[\log_{10}(\text{Re}_x)]^{2.58}} \quad (\text{Eq. 4})$$

For the hub-end region, the pressure drag due to the sudden end of the hub (base drag) was identified as an additional contribution to the skin-friction drag. A base drag correlation that is function of the Mach number was developed and used in the tool. The presence of struts, in the strut region, generate other additional drag sources such as the profile drag for the airfoil section, the incremental drag due to the pitched struts, and the interference drag which should capture the losses due to the proximity of the struts to the casing and the hub. These drag sources were developed and accounted for the overall drag calculation in the strut region.

The performance of the segmented diffuser was evaluated by calculating the pressure recovery

$$C_p = \frac{P_2 - P_1}{P_{t,1} - P_1} \quad (\text{Eq. 5})$$

and the total pressure loss coefficient along the diffuser

$$K = \frac{P_{t,1} - P_{t,2}}{P_{t,1} - P_1} \quad (\text{Eq. 6})$$

C. Results

The area calculations were first assessed and compared to CFD data to validate the geometry inputs. Figure 6 shows that the cross-sectional area calculations at the end surface of each region are comparable to the CFD results.

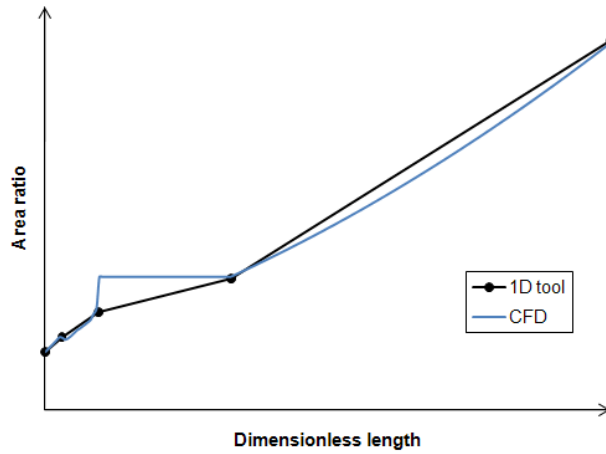


Figure 6. Comparison of Area Distributions along the ITSM Diffuser

Calculation of the pressure recovery at the diffuser exit revealed a low discrepancy of 0.04 % from the CFD result. It should be noted however that results obtained in regions preceding the conical segment were over-predicted, as it can be seen in Figure 7.

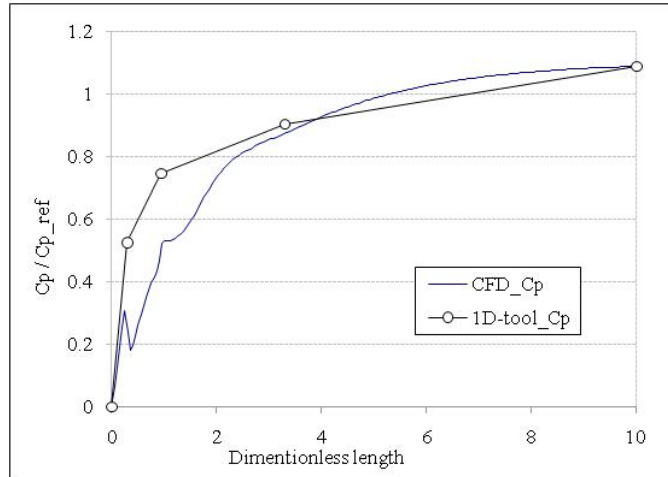


Figure 7. Comparison of Pressure Recoveries for the ITSM Diffuser

The exit plane of the annular region was chosen at proximity of the strut leading edge at the hub. Therefore, it is possible for the interference drag at the hub-strut intersect to also influence the boundary layer in the annular region, which the tool does not capture. Moreover, the tool area calculations do not account for the strut blockage. Axial velocity predictions, in regions where boundary layer growths are significant, greatly differ from the CFD results, as shown in Figure 8.

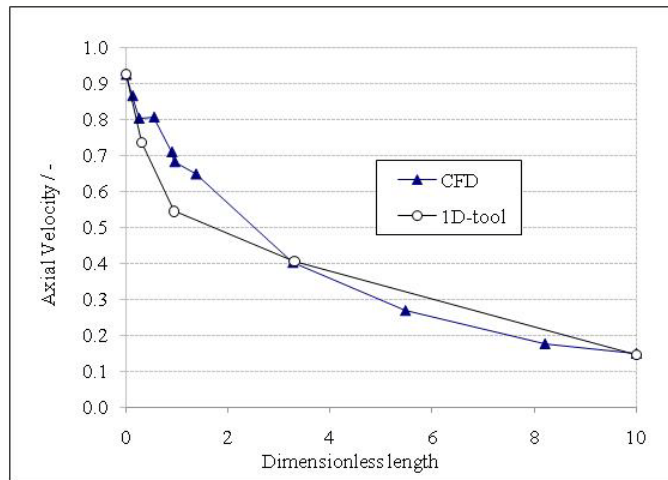


Figure 8. Comparison of Axial Velocities for ITSM Diffuser

D. Drag Correlations

The Exhaust diffuser was mostly segmented at locations where there was a change of the diffusion angle (kinks at casing and hub). To simplify calculations in the strut regions, the strut maximum thickness was assumed to be at the kink location. Furthermore, the

drag calculations used in the 1D tool are developed from Navy struts. In real engines, the strut airfoils do not necessarily have aerodynamic shapes. That is, correlations based on NACA profiles can be sources of under-prediction (or over-prediction) of the total drag on the struts.

An attempt to correct the total drag prediction in each region was conducted. The first step was to obtain CFD static pressure forces of the diffuser at similar locations as the tool. Next, it was thought that matching these forces to the values calculated by the tool, would generate new total drags that could be comparable to the CFD drag predictions. This reverse prediction would need to be applied to several diffuser configurations with different inlet profiles. The idea being it would be to obtain a more standard approximation of the drag, which would provide forged factors to values obtained in the 1D tool, as displayed in Figure 9.

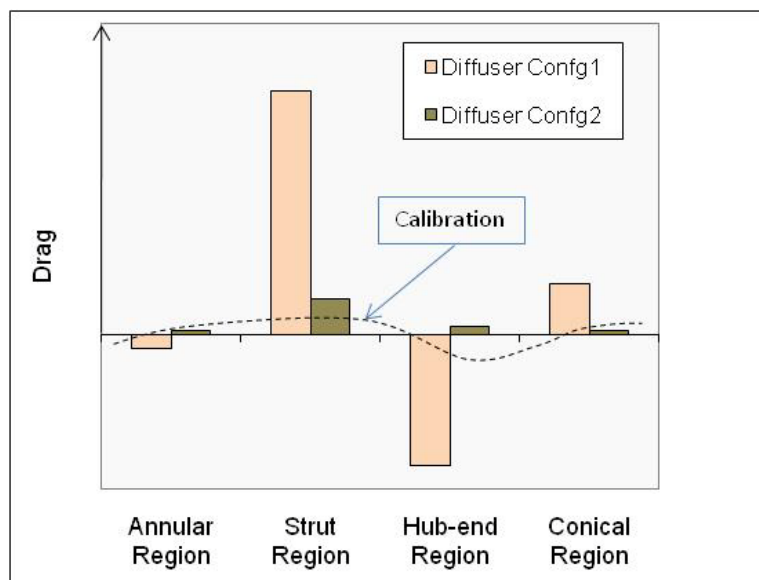


Figure 9. Drag Calibration Approach

E. Conclusion

The Strut region presented greater flow complexity compare to other regions. Additional post processing will be necessary to understand how the losses can be better modeled in these regions. Locations at which the 1D tool calculations are applied greatly influenced the results and comparisons to the CFD data, as it was observed in Figure 7. Therefore, an analysis on proper diffuser segmentation can be advantageous to improve the tool predictions. Regions where the flow was less complex such as annular and conical segments can be improved by adding boundary layer blockage in the 1D tool calculations.

ACKNOWLEDGEMENTS

I would like to express my gratitude to Siemens Energy, and specifically to the Orlando/Jupiter team, for making this opportunity a rewarding learning experience. As an intern at Siemens, I had the pleasure to be supervised by Dr. Ali Akturk and Dr. Jose Rodriguez. I would like to thank them for taking the time to teach me valuable engineering skills. Thank you to Dr. Matthew Montgomery and Dr. Chander Prakash for allowing me to be part of the Advanced Combustion & Aero-Thermal Technologies group and for broadening my knowledge of exhaust diffusers. Finally, thank you to the UTSR program. Without the program, this great opportunity would not have been possible.

REFERENCES

- [1] Japikse, D. and Baines, N. C., 1998, *Diffuser design technology*, Concepts ETI, Norwich, VT
- [2] Hirschmann, A., Volker, S., Casey, M., and Montgomery, M., 2012, “Hub extension in an axial gas turbine diffuser”, *Proceedings of ASME, Turbo Expo 2012, Copenhagen, Denmark*.
- [3] Volker, S., Kuschel, B., Hirschmann, A., Schatz, M., Casey, M., and Montgomery, M., 2012, “Hub injection flow control in a turbine exhaust diffuser”, *Proceedings of ASME, Turbo Expo 2012, Copenhagen, Denmark*.
- [4] Bertin, J. J., and Cummings, R. M., *Aerodynamics for engineers*, 5th Edition

APPENDIX

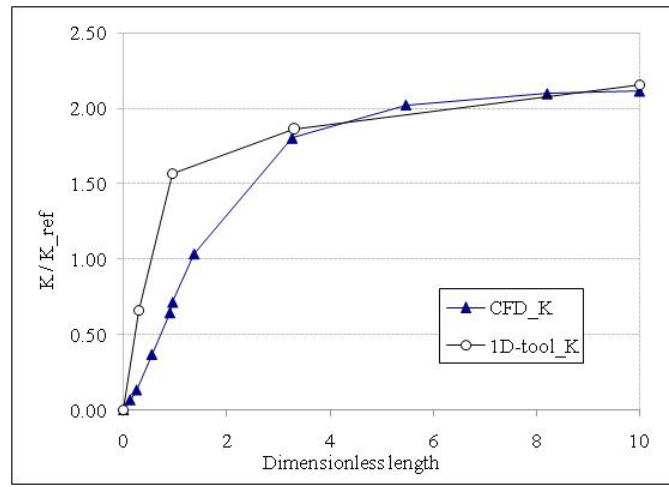


Figure 10. Comparison of Total Pressure Loss Coefficients for ITSM Diffuser

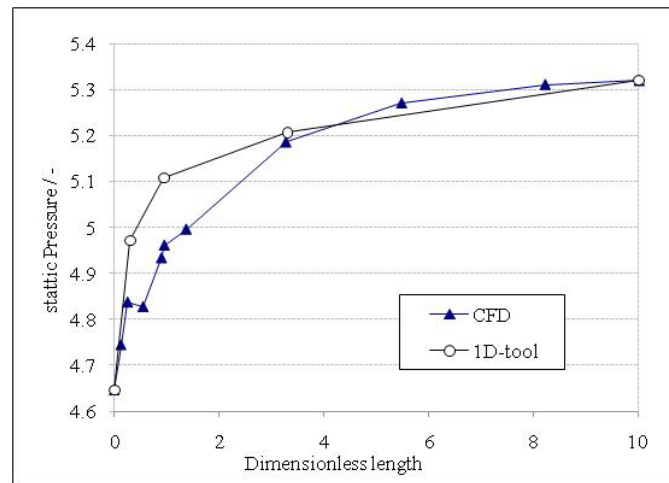


Figure 11. Comparison of Static Pressures for ITSM Diffuser

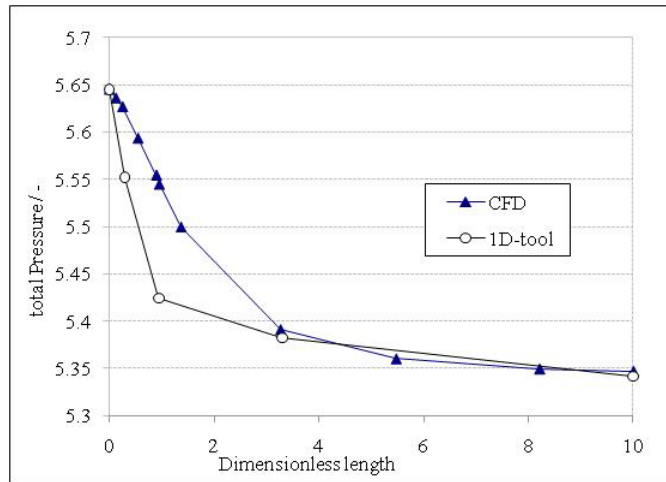


Figure 12. Comparison of Total Pressures for ITSM Diffuser